

# THERMODYNAMIC MODEL AND DATABASE FOR GASEOUS SPECIES IN MOLTEN OXIDE SLAGS

Youn-Bae Kang & Arthur Pelton

École Polytechnique, Canada

## ABSTRACT

*A thermodynamic model has been developed in the framework of the Modified Quasichemical Model in the quadruplet approximation in order to permit the calculation of solubilities of various gaseous species (sulfide, sulfate, nitride, carbide, water, etc.) in molten slags. The model calculates the solubilities from a knowledge of the thermodynamic activities of the component oxides and the Gibbs energies of the pure components (oxides, sulfides, sulfates, etc.). In particular, solubilities of sulfur as sulfide in the  $Al_2O_3$ -CaO-FeO-Fe<sub>2</sub>O<sub>3</sub>-MgO-MnO-Na<sub>2</sub>O-SiO<sub>2</sub>-TiO<sub>2</sub>-Ti<sub>2</sub>O<sub>3</sub> multi-component slag, predicted from the present model with no adjustable model parameters, were found to be in good agreement with all available experimental data. The model applies at all compositions from pure oxides to pure sulfides, sulfates, etc., and from basic slags to acidic slags. By coupling this database with other evaluated databases for molten steel and gaseous phases, practically important slag/steel/gas equilibria can be computed such as the S-distribution ratio and gas impurity pick-up levels in molten steel.*

## INTRODUCTION

Various gaseous species like S, N, C and H dissolve in molten slags as sulfide, sulfate, nitride, carbide, carbonate, etc. Knowledge of the solubility of these gaseous species in slags is very important. For example, control of the sulfur level in many grades of commercial products such as steel, copper and lead can be achieved by control of the distribution ratio of sulfur between the liquid metals and the molten slags. Usually a low sulfur content is desired due to its detrimental effect on many types of final steel products. On the other hand, a relatively high sulfur content is desired in some steel grades such as fast-cutting steels.

Approaches have been proposed to correlate the sulfide capacity with the optical basicity [38], or bulk composition [28] of slags. These approaches require many empirical model parameters and have low predictive ability. A more fundamental approach was proposed by Gaye and Lehmann [14] who included sulfide solubility in the IRSID cell model. This approach has been more successful, but still requires a number of empirical parameters.

In the model of Reddy and Blander [33], later modified by Pelton *et al.* [30], the activity of sulfide in the slags is calculated from considerations of its configurational entropy of mixing with the silicate structural units, while the activities of the oxide components of the slag are taken from existing evaluated databases. This model yields good predictions of Cs in multicomponent slags, with no adjustable model parameters. The model has been extended [31] with equal success to the dissolution of other species ( $\text{SO}_4^{2-}$ ,  $\text{CO}_3^{2-}$ ,  $\text{I}^-$ , etc.).

In the present article we report on a recent general model for the solubility of gaseous species in molten slags within the framework of the Modified Quasichemical Model (MQM) in the quadruplet approximation [32]. This model is similar to the Reddy-Blander-Pelton (R-B-P) model inasmuch as the sulfide activities are calculated from considerations of the entropy of structural units, while the oxide activities are taken from the existing extensive evaluated thermodynamic database which we have developed over the last 30 years. Like the R-B-P model, the model involves no adjustable parameters. The model is superior to the R-B-P model inasmuch as it applies even in highly acidic slags and even at very high sulfide contents, and its general predictive ability is even better. The model has been incorporated into the FactSage [3] databases and software.

## THERMODYNAMIC MODEL

It is assumed that the molten oxide containing sulfur consists of two sublattices:  $(\text{Ca}^{2+}, \text{Mg}^{2+}, \text{Si}^{4+}, \text{Al}^{3+}, \dots)[\text{O}^{2-}, \text{S}^{2-}]$ . Cations such as  $\text{Ca}^{2+}$ ,  $\text{Mg}^{2+}$ ,  $\text{Si}^{4+}$ ,  $\text{Al}^{3+}$  etc. reside exclusively on the cationic sublattice, while anions such as  $\text{O}^{2-}$  and  $\text{S}^{2-}$  reside exclusively on the anionic sublattice.

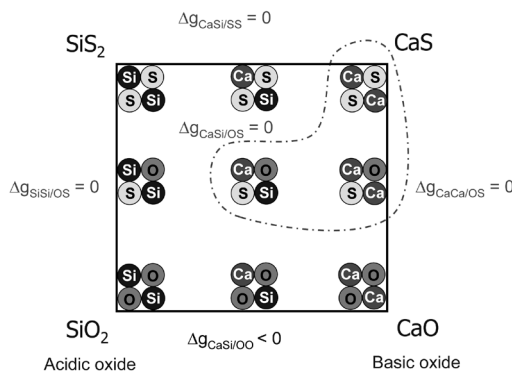
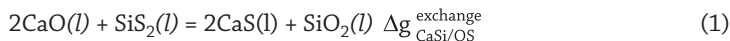


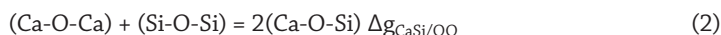
Figure 1: Quadruplets in  $\text{CaO-SiO}_2\text{-CaS-SiS}_2$  slags. The three quadruplets within the dashed line are the major S-containing quadruplets

Consider a CaO-SiO<sub>2</sub> slag containing S. In Figure 1, a schematic composition square is shown for this reciprocal slag system. The following two reactions must be considered in the model. The first is the exchange reaction among the liquid components:



If  $\Delta g_{\text{CaSi/OS}}^{\text{exchange}}$  is negative, then Reaction (1) is displaced to the right. This reaction determines the first nearest-neighbor (FNN) short-range-ordering (SRO) in the slag. Since  $\Delta g_{\text{CaSi/OS}}^{\text{exchange}}$  among the pure liquid components is of the order of  $\sim -400$  kJ/mol, the FNN SRO is extremely strong, with Ca-S and Si-O pairs being strongly favoured over Ca-O and Si-S pairs.

Secondly, it is well-known that molten oxides often show very strong second-nearest neighbor (SNN) SRO between cations. For example, in CaO-SiO<sub>2</sub> slags, the maximum SNN SRO occurs near the Ca<sub>2</sub>SiO<sub>4</sub> composition where nearly all Si<sup>4+</sup> cations have Ca<sup>2+</sup> cations in their second coordination shell (equivalent to a model of Ca<sup>2+</sup> cations and SiO<sub>4</sub><sup>4-</sup> orthosilicate anions.) This is taken into account by the following SNN pair exchange reaction:



For many molten oxide systems, the Gibbs energy changes of these pair exchange reactions are very negative (e.g.,  $\Delta g_{\text{CaSi/OO}} = \sim -60$  kJ/mol) and SNN SRO is consequently very important. Moreover, the coupling of the FNN SRO and SNN SRO must be taken into account in the thermodynamic modeling.

In order to model the Gibbs energy of two-sublattice reciprocal ionic liquids with simultaneous FNN and SNN SRO, a Modified Quasichemical Model in the quadruplet approximation was developed by Pelton *et al.* [32] and has been successfully applied in molten salt system [8, 9, 10, 24]. In this model, nine quadruplet clusters are defined for CaO-SiO<sub>2</sub>-CaS-SiS<sub>2</sub> slags as shown in Figure 1. These *quadruplets* are distributed randomly over quadruplet sites. Hence, the SNN pairs shown in Reaction (2) are associated with the quadruplets CaCa/OO, SiSi/OO, and CaSi/OO. A complete mathematical description of the model is given in [32].

The Gibbs energies of the quadruplets corresponding to the pure components (SiO<sub>2</sub>, CaO, CaS, SiS<sub>2</sub>, ...) are equal to the standard Gibbs energies of the components, and are taken from standard compilations [39]. The Gibbs energies of the binary oxide quadruplet clusters such as CaSi/OO are given by the parameters  $\Delta g_{ij/OO}$  (center of lower edge of Figure 1). These parameters are taken from the FACT molten oxide database of MQM parameters. This database has been developed in the authors' research group over the last 30 years by critical evaluation of all available thermodynamic and phase equilibrium data for the Al<sub>2</sub>O<sub>3</sub>-CaO-FeO-Fe<sub>2</sub>O<sub>3</sub>-MgO-MnO-Na<sub>2</sub>O-SiO<sub>2</sub>-TiO<sub>2</sub>-Ti<sub>2</sub>O<sub>3</sub> systems. The Gibbs energies of formation  $\Delta g_{ij/SS}$  and  $\Delta g_{ii/OS}$  of the quadruplets (on the right, left and upper edges of Figure 1) are assumed to be zero. That is, these binary systems are assumed to be close to ideal. These Gibbs energies could be treated as adjustable model parameters which could be optimized to give the best fit to available data for sulfide capacities. However, we have found that the calculations are relatively insensitive to these parameters, and very good predictions are obtained by simply setting them all to zero. Finally, the Gibbs energy of formation of the central *reciprocal* quadruplets (*ij/OS* in Figure 1) from the binary quadruplets are also assumed to be zero. The coordination numbers of all species are fixed by the ionic charges and positions of maximum SRO as explained in [32].

That is, the present model requires no new adjustable model parameters in order to predict the solubilities of gaseous species in molten slags.

## SULFIDE CAPACITY

At low oxygen partial pressure, sulfur dissolves in molten slags as sulfide ( $S^{2-}$ ). When the sulfide concentration is small, the sulfide capacity, defined as  $C_s = (wt\%S)(p_{O_2}/p_{S_2})^{1/2}$  is approximately independent of the sulfur content. Many investigations have been conducted to measure the sulfide capacities of various slags over the years. In the present study, we have considered all available literature data for  $Al_2O_3$ -CaO-FeO- $Fe_2O_3$ -MgO-MnO- $Na_2O$ - $SiO_2$ - $TiO_2$ - $Ti_2O_3$  slags, and have compared these data with the predictions of the present model. Good agreement within experimental error limits was obtained in nearly all cases.

Selected comparisons are shown in the following figures. Sulfide capacities in binary CaO- $SiO_2$ , MnO- $SiO_2$  and CaO- $Al_2O_3$  slags are shown in Figures 2 to 4 respectively. The composition and temperature dependence of  $C_s$  and predicted by the model, within experimental error limits, with no adjustable model parameters. (Dotted lines in Figures 2 to 4 indicate sub-liquidus compositions.)

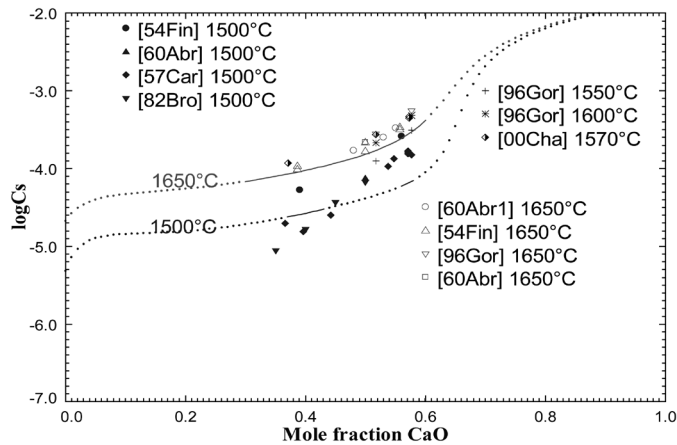


Figure 2: Calculated sulfide capacity in CaO- $SiO_2$  slags at  $p_{O_2} = 10^{-9}$  bar,  $p_{S_2} = 10^{-2}$  bar compared with experimental data

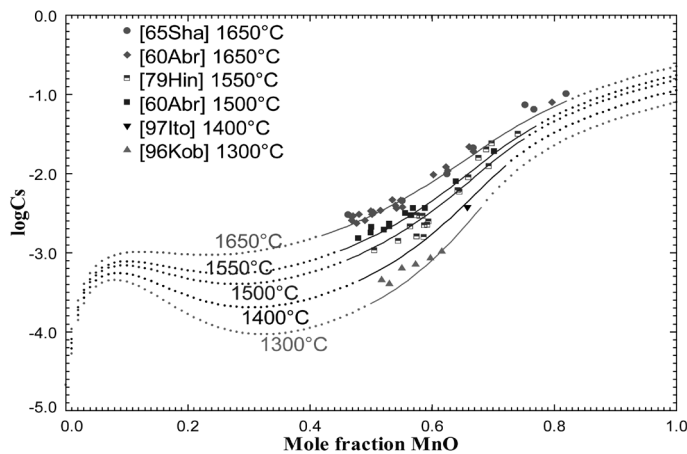


Figure 3: Calculated sulfide capacity in MnO- $SiO_2$  slags at  $p_{O_2} = 10^{-8}$  bar,  $p_{S_2} = 10^{-6}$  bar compared with experimental data

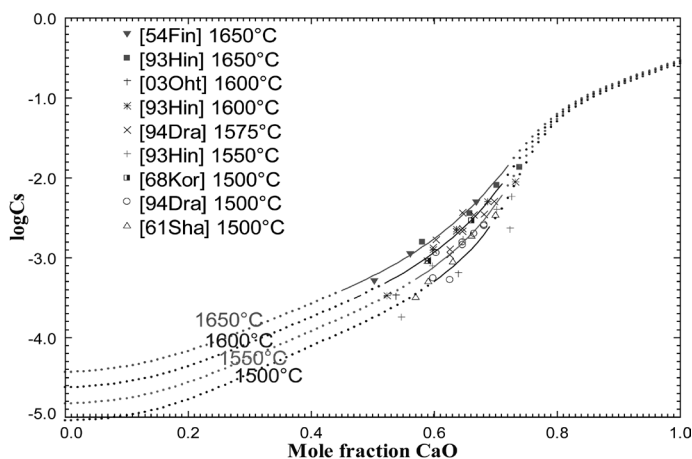


Figure 4: Calculated sulfide capacity in  $\text{CaO-Al}_2\text{O}_3$  slags at  $p_{\text{O}_2} = 10^{-7}$  bar,  $p_{\text{S}_2} = 10^{-3}$  bar compared with experimental data

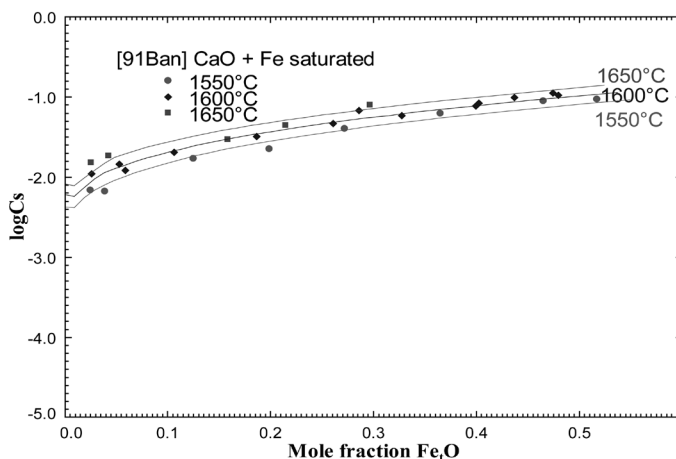


Figure 5: Calculated sulfide capacity in  $\text{CaO-FeO-Al}_2\text{O}_3$  slags at CaO/Fe co-saturation compared with experimental data

The present model can easily be extended to ternary and multicomponent slags. Full details are given in reference [32]. Selected comparisons of the predictions of the model with experimental data are shown in Figures 5 to 8. Figure 8 illustrates that the current model applies not only at low sulfide concentrations but, in fact, at all compositions up to pure sulfide. Although there is disagreement between the calculations and some of the experimental points of Hasegawa *et al.* [16] in Figure 8, the calculations are in excellent agreement with the more recent experimental data of Woo *et al.* [41] which are presented at this Conference.

The agreement between the model predictions and the experimental data in Figures 5 to 8 is within, or nearly within, the experimental error limits in all cases. The agreement could be improved, of course, through the addition of adjustable model parameters. However, it is our intention here to show the accuracy of the predictions when no adjustable parameters whatsoever are used.

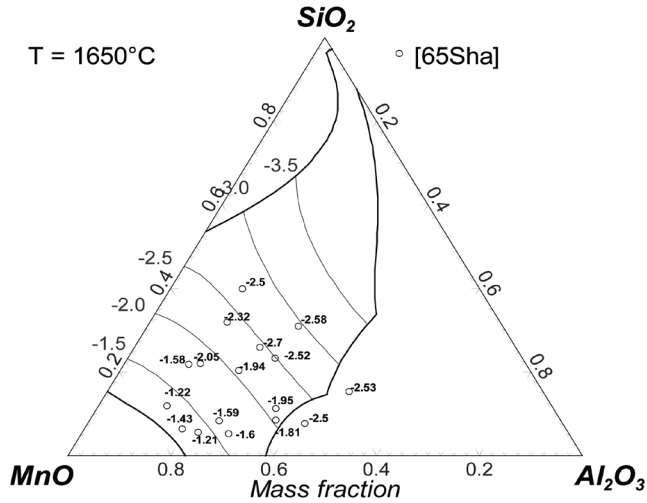


Figure 6: Calculated iso-Cs lines in MnO-Al<sub>2</sub>O<sub>3</sub>-SiO<sub>2</sub> slags at  $p_{O_2} = 10^{-7}$  bar,  $p_{S_2} = 10^{-3}$  bar compared with experimental data. Numbers adjacent to lines and symbols are log Cs

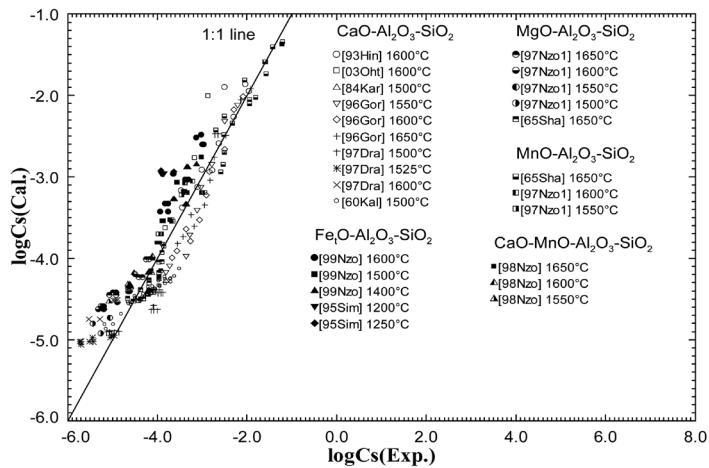


Figure 7: Agreement between experimental and predicted sulfide capacities for MO-NO-...-Al<sub>2</sub>O<sub>3</sub>-SiO<sub>2</sub> multicomponent slags

## APPLICATION TO STEEL REFINING

The sulfur distribution ratio ( $L_s = (wt\%S)_{slag} / [wt\%S]_{steel}$ ) is an important factor during the steel refining process. With commercial software such as FactSage, with the present model, and with a thermodynamic database for molten steel,  $L_s$  can readily be calculated. In Figure 9 is shown an example of such a calculation for a CaO-SiO<sub>2</sub>-Al<sub>2</sub>O<sub>3</sub> slag in equilibrium with an Fe-0.1C-0.7Mn-0.1Si-0.05Al-0.005O-0.003S (wt%) steel at 1600°C. As can be seen,  $L_s$  is highest for CaO-saturated, low-SiO<sub>2</sub> slags, which is the composition range of widely-used refining slags.

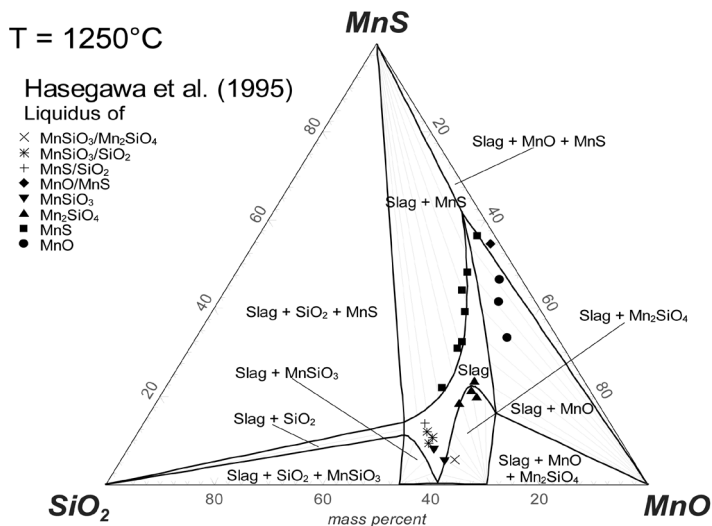


Figure 8: Predicted phase diagram of the MnO-SiO<sub>2</sub>-MnS system at 1250°C compared with experimental data

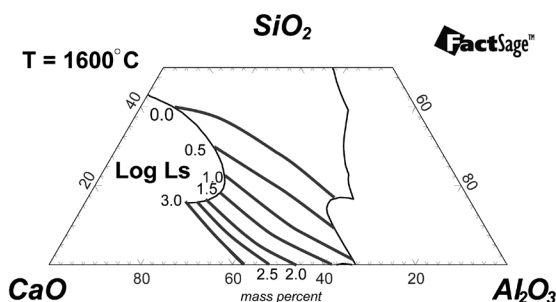


Figure 9: Predicted S-distribution ratio ( $L_s = (wt\%S)_{slag} / [wt\%S]_{steel}$ ) for a CaO-SiO<sub>2</sub>-Al<sub>2</sub>O<sub>3</sub> slag at 1600°C in equilibrium with a steel of the composition 0.1C-0.7Mn-0.1Si-0.05Al-0.0050-0.003S (wt%)

## OTHER GASEOUS SPECIES: SULFATE, NITRIDE, CARBIDE, WATER, ETC.

A similar approach can be used to model solubilities in oxide slags of other gaseous species such as sulfate, nitride, carbide, water, etc. For example, water dissolution in CaO-Al<sub>2</sub>O<sub>3</sub> slags has been modeled as  $(Ca^{2+}, Al^{3+}, H^+)(O^{2-}, OH^-)$ . Calculated water capacities defined as  $C_{H_2O} = (wt\%H_2O) \times (pH_2O)^{1/2}$  are compared with available experimental data in Figure 10. Again, good agreement is observed. Similar good agreement has been obtained for the solubilities of other gases.

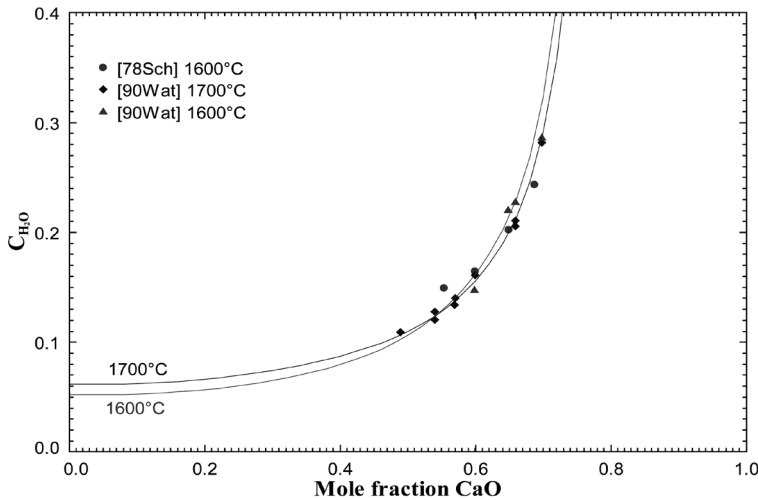


Figure 10: Calculated water capacity in CaO-Al<sub>2</sub>O<sub>3</sub> slags at  $p_{\text{H}_2\text{O}} = 0.3$  bar compared with experimental data

## CONCLUSIONS

A general thermodynamic model has been developed to describe the solubility in molten oxide slags of gaseous species such as sulfide, sulfate, nitride, carbide, water, etc., using the Modified Quasichemical Model in the quadruplet approximation. This model takes into account first-nearest-neighbor and second-nearest-neighbor short-range-ordering simultaneously. The model takes the activities of the oxide components from an existing evaluated thermodynamic database for oxide slags. Gibbs energies of pure liquid component sulfides are taken from standard compilations. With no other model parameters, predictions of sulfide capacities, within or nearly within experimental error limits, are obtained with all literature data for Al<sub>2</sub>O<sub>3</sub>-CaO-FeO-Fe<sub>2</sub>O<sub>3</sub>-MgO-MnO-Na<sub>2</sub>O-SiO<sub>2</sub>-TiO<sub>2</sub>-Ti<sub>2</sub>O<sub>3</sub> slags. The model applies at sulfide contents up to pure liquid sulfides and from highly basic to highly acidic slags. Similar good agreement with experimental data is found when the model is applied to predict the solubilities of sulfate, halides, carbonate, etc. in molten oxide slags.

## ACKNOWLEDGEMENTS

This study was supported by a grant from the Fundamental R&D Program for Core Technology of Materials funded by the Ministry of Commerce, Industry and Energy, Republic of Korea.

## REFERENCES

- Abraham, K. P., *et al.* (1960). *Sulfide Capacities of Silicate Melts – Part I*. J. Iron and Steel Inst., 196, pp. 309-312. [1]
- Abraham, K. P. & Richardson, F. D. (1960). *Sulfide Capacities of Silicate Melts – Part II*. J. Iron and Steel Inst., 196, pp. 313-317. [2]

- Bale, C., et al.** (2002). *FactSage Thermochemical Software and Databases*. Calphad 26, pp.189-228.; www.factsage.com. [3]
- Ban-Ya, S., et al.** (1991). *O, P and S Distribution Equilibria between Liquid Iron and CaO-Al<sub>2</sub>O<sub>3</sub>-FetO Slag Saturated with CaO*. Tetsu-to-Hagane, 77, pp. 361-368. [4]
- Brown, S. D., et al.** (1982). *Sulfide Capacity of Titania-Containing Slags*. Ironmaking and Steel-making, 9, pp. 163-167. [5]
- Carter, P. T. & Macfarlane, T. G.** (1957). *The Thermodynamic Properties of CaO-SiO<sub>2</sub> Slags*. J. Iron and Steel Inst., 185, pp. 62-66. [6]
- Chapman, M., et al.** (2000). *Sulfide Capacity of Titania Containing Slags*. Elektrometallurgiya, pp. 34-39. [7]
- Chartrand, P. & Pelton, A. D.** (2001). *Thermodynamic Evaluation and Optimization of the Li, Na, K, Mg, Ca//F, Cl Reciprocal System Using the Modified Quasichemical Model*. Metall. Mater. Trans. A, 32A, pp. 1417-1430. [8]
- Chartrand, P. & Pelton, A. D.** (2002). *A Predictive Thermodynamic Model for the Al-NaF-AlF<sub>3</sub>-CaF<sub>2</sub>-Al<sub>2</sub>O<sub>3</sub> System*. Light Metals 2002, pp. 245-252. [9]
- Coursol, P., et al.** (2005). *The Ca(SO<sub>4</sub>)-Na<sub>2</sub>(SO<sub>4</sub>)-Ca<sub>3</sub>(AsO<sub>4</sub>)<sub>2</sub>-Na<sub>3</sub>(AsO<sub>4</sub>) Phase Diagram*. Metall. Mater. Trans B. 36B, pp. 825-836. [10]
- Drakaliysky, E., et al.** (1994). *Sulphide Capacities of CaO-Al<sub>2</sub>O<sub>3</sub> Slags in the Temperature Range 1773-1848K*. High Temp. Mater. Process., 23, pp. 263-272. [11]
- Drakaliysky, E., et al.** (1997). *An Experimental Study of the Sulfide Capacities in the System Al<sub>2</sub>O<sub>3</sub>-CaO-SiO<sub>2</sub>*. Can. Metall. Quarter., 36, pp. 115-120. [12]
- Fincham, C. J. B. & Richardson, F. D.** (1954). *The Behavior of Sulphur in Silicate and Aluminate Melts*. Proc. R. Soc., London, 223A, pp. 40-62. [13]
- Gaye, H. & Lehmann, J.** (1996). *Modeling of Slag Thermodynamic Properties. From Oxides to Oxisulphides*. Proc. 5<sup>th</sup> Int. Conf. on Molten Slags, Fluxes and Salts, pp. 27-34. [14]
- Gornerup, M. & Wijk, O.** (1996). *Sulphide Capacities of CaO-Al<sub>2</sub>O<sub>3</sub>-SiO<sub>2</sub> Slags at 1550, 1600 and 1650°C*. Scand. J. Metall., 25, pp. 103-107. [15]
- Hasegawa, A., et al.** (1995). *Phase Equilibria for the MnO-SiO<sub>2</sub>-MnS Slag System*. Tetsu-to-Hagane, 81, pp. 1109-1113. [16]
- Hino, M. & Fuwa, T.** (1979). *Sulphide Capacity of Liquid Manganese Silicate*. Proc. 3<sup>rd</sup> Int. Iron and Steel Conr. (1979) ASM International, Materials Park, OH, pp. 321-326. [17]
- Hino, M., et al.** (1993). *Sulfide Capacities of CaO-Al<sub>2</sub>O<sub>3</sub>-MgO and CaO-Al<sub>2</sub>O<sub>3</sub>-SiO<sub>2</sub> Slags*. ISIJ Int., 33, pp. 36-42. [18]
- Ito, M., et al.** (1997). *Thermodynamics of the MnO-SiO<sub>2</sub>-TiO<sub>2</sub> System at 1673 K*. ISIJ Int., 37, pp. 839-843. [19]
- Kalyanram, M. R., et al.** (1960). *The Activity of Calcium Oxide in Slags in the Systems CaO-MgO-SiO<sub>2</sub>, CaO-Al<sub>2</sub>O<sub>3</sub>-SiO<sub>2</sub>, and CaO-MgO-Al<sub>2</sub>O<sub>3</sub>-SiO<sub>2</sub> at 1500°C*. J. Iron and Steel Inst., 195, pp. 58-64. [20]
- Karsrud, K.** (1984). *Sulphide Capacities of Synthetic Blast Furnace Slags at 1500°C*. Scand. J. Metall., 13, pp. 144-150. [21]

- Kor, G. J. W. & Richardson, F. D.** (1968). *Sulphur in Lime-Alumina Mixtures*. J. Iron and Steel Inst., 206, pp. 700-704. [22]
- Kobayashi, T., et al.** (1996). *Thermodynamics of Sulfur in the BaO-MnO-SiO<sub>2</sub> Flux System*, Metall. Mater. Trans. B, 27B, pp. 652-657. [23]
- Lindberg, D., et al.** (2006). *Thermodynamic Evaluation and Optimization of the (Na + K + S) System*. J. Chem. Thermodynamics, 38, pp. 900-915. [24]
- Nzotta, M.** (1997). *Sulfide Capacities in MgO-SiO<sub>2</sub> and CaO-MgO-SiO<sub>2</sub> Slags*. Scand. J. Metall., 26, pp. 169-177. [25]
- Nzotta, M. M., et al.** (1998). *Sulfide Capacities in some Multi Component Slag Systems*. ISIJ Int., 38, pp. 1170-1179. [26]
- Nzotta, M.M., et al.** (1999). *A Study of the Sulfide Capacities of Iron-Oxide Containing Slags*. Metall. Trans. B., 30B, pp. 909-920. [27]
- Nzotta, M. M., et al.** (2000). *A Study on the Sulfide Capacities of Steelmaking Slags*, Scand. J. Metall. 29, pp. 177-184. [28]
- Ohta, M., et al.** (2003). *Effects of CaF<sub>2</sub>, MgO and SiO<sub>2</sub> Addition on Sulfide Capacities of the CaO-Al<sub>2</sub>O<sub>3</sub> Slag*. Tetsu-to-Hagane, 89, pp.742-749. [29]
- Pelton, A. D., et al.** (1993). *Calculation of Sulfide Capacities of Multicomponent Slags*. Metall. Trans. B. 24B, pp. 817-825. [30]
- Pelton, A. D.** (1999). *Thermodynamic Calculation of Gas Solubilities in Oxide Melts and Glasses*. Glastechn. Ber. 72, pp. 214-226. [31]
- Pelton, A. D., et al.** (2001). *The Modified Quasichemical Model IV - Two Sublattice Quadruplet Approximation*. Metall. Mater. A. 32A, pp. 1409-1416. [32]
- Reddy, R. G. & Blander, M.** (1987). *Modeling Sulfide Capacities of Silicate Melts*. Metall. Trans. B 18B, pp. 591-569. [33]
- Schwerdtfeger, K. & Schubert, H. G.** (1978). *Solubility of Water in CaO-Al<sub>2</sub>O<sub>3</sub> Melts at 1600°C*. Metall. Trans B. 9B, pp. 143-144. [34]
- Sharma, R. A. & Richardson F. D.** (1961). *Activities in Lime-Alumina Melts*. J. Iron and Steel Inst., 198, pp. 386-390. [35]
- Sharma, R.A. & Richardson, F.D.** (1965). *Activities of Manganese Oxide, Sulfide Capacities, and Activity Coefficients in Aluminate and Silicate Melts*. Trans. Met. Soc. AIME, 223, pp. 1586-1592. [36]
- Simeonov, S. R., et al.** (1995). *Sulfide Capacities of Fayalite-Base Slags*. Metall. Trans. B., 26B, pp. 325-334. [37]
- Sosinsky, D. J. & Sommerville, I.D.** (1986). *The Composition and Temperature Dependence of the Sulfide Capacity of Metallurgical Slags*. Metall. Trans. 17B, pp. 331-337. [38]
- Stull, D. R. & Prophet, H.** (1985). *JANAF Thermochemical Tables*. U.S. Department of Commerce, Washington. [39]
- Watanabe, M. et al.** (1990). *Dissolution of Water Vapor in Liquid Aluminates*. Tetsu-to-Hagane, 76, pp. 1672-1679. [40]
- Woo, et al.** (2008). *Experimental Investigation of Phase Equilibria in the MnO-SiO<sub>2</sub>-Al<sub>2</sub>O<sub>3</sub>-MnS System*. Proc. 8<sup>th</sup> Int. Conf. on Molten Slags, Fluxes and Salts, Santiago, Chile. [41]